

# Simultaneous Station and Formation Keeping Using Solar Radiation

## Pressure in Artificial Halo Orbit about the SEL2 Point

Keisuke Sugiura (Aoyama Gakuin University), Ahmed Kiyoshi Sugihara (JAXA), Yuki Takao (JAXA),  
Yoshiki Sugawara (Aoyama Gakuin University) and Osamu Mori (JAXA)

In optical astronomy, physically achievable spatial resolution is limited by the physical telescope size, i.e. the diffraction limit. However, launching very large telescopes into space is impractical, therefore, interferometric observations using satellite formation flight are often proposed. In order to obtain an image with an interferometer, it is necessary to change the distance and relative orientation between the telescopes during the observation. In conventional formation flight interferometers, fuel is consumed in this process. In this work, the authors propose to place a formation flight interferometer on an artificial halo orbit around the Sun-Earth L2 orbit, in which the solar radiation pressure is used as the only control input. With this suggestion, it is expected to realize the maintenance control of the artificial halo orbit and relative position control without consuming fuel.

### 太陽-地球系 L2 点近傍におけるフォーメーションフライトでの太陽輻射圧を利用した相対位置制御と小円ハロー軌道の維持について

宇宙機のフォーメーションフライトは大型の宇宙機の機能を小型の宇宙機に分散させるという概念である。この手法は大型望遠鏡の機能を分散した干渉計観測と親和性が高い。干渉計観測で像を得るためには、観測中に望遠鏡同士の距離を変える必要がある。従来の検討ではこの過程で燃料を消費してきた。そこで、本研究では、観測中に推進剤を使用せずにフォーメーションフライトを制御することを提案する。具体的には制御入力に太陽輻射圧を用い、太陽-地球系第2ラグランジュ点周りの基準軌道維持とフォーメーションの相対位置の同時制御を行う。

## 1. Introduction

In recent years, the performance of telescopes on Earth has been approaching its limits due to diffraction limitations and atmospheric diffusion. Therefore, higher performance can only be achieved by placing larger telescopes in space. However, it is not practical to launch a large telescope. Therefore, as a distributed approach, interferometric observation using satellite formation flights is considered to be a promising method. In interferometric observations, multiple telescopes are placed at different distances and the signals received by each telescope are combined to obtain an image of the celestial body. From the principle of interferometry, it is possible to estimate

the luminance distribution of a celestial body by collecting various baseline vectors. Here, the various baseline vectors mean that the vectors connecting the telescopes have various directions and lengths. In order to perform interferometric observations with satellites, it is necessary to design a formation flight orbit in which two satellites collect various baseline vectors. In conventional formation flight interferometry studies, fuel is consumed in this process.

This study proposes a fuel-free orbit by placing the interferometric observations in formation flights around the second Lagrange point of the Sun-Earth system (SEL2). The Lagrange points are the five stationary solutions of the circularly restricted three-body problem. They are known to be a dynamically equilibrium points. This characteristic indicates that

the thrust required to maintain the orbit and change the formation size is small. Therefore, the use of solar radiation pressure (SRP), which is a small thrust force, as a control input is considered to be able to control the orbit without using fuel. In fact, many studies on station keeping and formation keeping using SRP around Lagrange points have been carried out to date, including Bookless and McInnes [1], Shehid [2], etc. However, the reference orbit that has been the subject of these studies is a halo orbit. The halo orbit requires less control input to maintain, but the size of the orbit is about 1 million kilometers. One advantage of conducting interferometric observations around the Lagrange point is that the thermal and communication environments are stable. These can be further stabilized by designing a halo orbit with a reduced radius. Taro [3] investigated the possibility of reducing the size of the halo orbit arbitrarily. Tanaka [4] showed that the thrust to maintain the orbit can be provided by SRP. This orbit is called a small-circle halo orbit (SCHO), it can be conceptually represented as shown in Figure 1, which shows that it is an orbit that can make the best use of the advantages of SEL2. However, few researchers have studied formation flight with SEL2 using SCHO as a reference orbit. In this study, a SCHO is designed as a reference orbit, and two satellites are designed to orbit around it to obtain a baseline vector suitable for interferometric observations. Furthermore, the purpose is to maintain a SCHO and simultaneously control the relative position when only the acceleration due to SRP is used as a control input. Since the acceleration by SRP can be controlled by the attitude of the spacecraft toward the sun, the attitude of the spacecraft is used as the control input in this study.

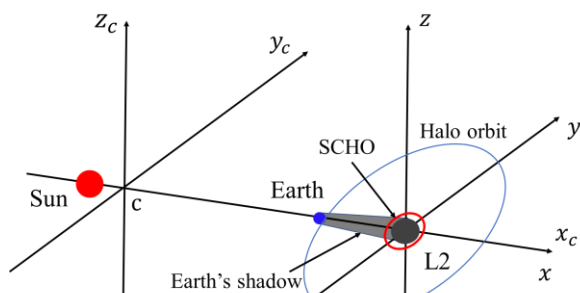


Fig. 1. Concept of SCHO and halo orbit around SEL2.

## 2. Orbit Design

### 2.1 Dynamics of System

In this chapter, the SCHO and formation flight relative orbit around SEL2 will be designed. First, the definition of coordinates is shown in Figure 2. In this study, the circular restricted three-body problem is used to describe the motion around SEL2. Its equation of motion is expressed as

$$\begin{aligned}\ddot{x} - 2\dot{y} &= -\frac{\partial \bar{U}}{\partial x} + a_x \\ \ddot{y} + 2\dot{x} &= -\frac{\partial \bar{U}}{\partial y} + a_y\end{aligned}\quad (1)$$

$$\begin{aligned}\ddot{z} &= -\frac{\partial \bar{U}}{\partial z} + a_z \\ \bar{U} &= -\frac{1}{2}((x+1-\mu+\gamma_2)^2 + y^2) \\ &\quad - \left( \frac{1-\mu}{r_S} + \frac{\mu}{r_E} \right)\end{aligned}\quad (2)$$

$$r_S = \sqrt{(x+1+\gamma)^2 + y^2 + z^2}\quad (3)$$

$$r_E = \sqrt{(x+\gamma)^2 + y^2 + z^2}$$

Here,  $\gamma_2$  is the distance from the Earth to the SEL2,  $r_S$  is the distance from the Sun, and  $r_E$  is the distance from the Earth to the satellite. The linearized equation of motion is expressed as follows [4].

$$\begin{aligned}\ddot{x} - 2\dot{y} - (1+2c_2)x &= a_x \\ \ddot{y} + 2\dot{x} + (c_2-1)y &= a_y\end{aligned}\quad (4)$$

$$\ddot{z} + c_2z = a_z$$

$$c_2 = \frac{1}{\gamma^3} \left( \mu + \frac{(1-\mu)\gamma^3}{(1+\gamma)^3} \right)\quad (5)$$

The right-hand side is the acceleration of each axis, and the left-hand side,  $c_2$ , is a constant. From Eq. (4), in the orbit design of the circular restricted three-body problem, an arbitrary orbit is first designed. The acceleration input required to create the orbit is roughly obtained by substituting it into the linear equation of motion. Next, the obtained acceleration is expressed in terms of the satellite attitude angle to be realized in SRP.

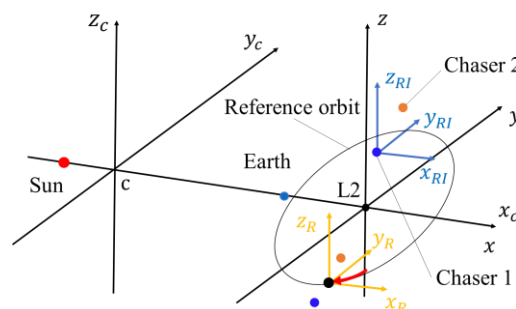


Fig. 2. Coordinate definition.

## 2.2 Formulation of Solar Radiation Pressure

The SRP of a spacecraft depends mainly on the satellite mass, area, optical characteristics of the satellite surface, and attitude angle. The optical properties can be divided into three attributes, which are assigned as Table 1. Optical properties are based on the IKAROS parameters [5]. The acceleration by SRP is expressed by Eq. (6) [4]. Here, the attitude angle is defined as shown in Fig. 3. The  $\mathbf{s}$  in Eq. (6) is the unit direction vector from the spacecraft to the Sun. The radius of the orbit length of the SCHO is much smaller than the distance from the Sun to the SEL2, it can be approximated as Eq. (7).

$$\mathbf{a}_{srp} = -\frac{PA}{m}(\mathbf{s} \cdot \mathbf{n}) \left[ (C_{abs} + C_{dif})\mathbf{s} + \left( \frac{2}{3}C_{dif} + 2(\mathbf{s} \cdot \mathbf{n})C_{spe} \right)\mathbf{n} \right] \quad (6)$$

$$\mathbf{s} \approx \begin{bmatrix} -1 \\ 0 \\ 0 \end{bmatrix} \quad (7)$$

Also,  $\mathbf{n}$  is the unit normal vector from the surface of the spacecraft when the spacecraft is a flat panel model. This can be written as Eq. (8) depending on the attitude angle  $\psi$  and  $\phi$ . If  $\psi$  and  $\phi$  are approximated as small, it can be rewritten as

$$\mathbf{n} = \begin{bmatrix} -\cos\phi \cos\psi \\ -\cos\phi \sin\psi \\ \sin\phi \end{bmatrix} \approx \begin{bmatrix} -1 \\ -\psi \\ \phi \end{bmatrix} \quad (8)$$

From the above, Eq. (6) can be rearranged by substituting  $\mathbf{s}$  and  $\mathbf{n}$ . The acceleration due to SRP can be expressed in conjunction with the attitude angle as shown in Eq. (9).

$$\mathbf{a}_{srp} \approx \begin{bmatrix} k_1 \\ k_2\psi \\ -k_2\phi \end{bmatrix} \quad (9)$$

where  $k_1$  and  $k_2$  are constants formed by the optical properties as

$$k_1 = \frac{PA}{m} \left( C_{abs} + \frac{5}{3}C_{dif} + 2C_{spe} \right) \quad (10)$$

$$k_2 = \frac{PA}{m} \left( \frac{2}{3}C_{dif} + 2C_{spe} \right)$$

Substituting Eq. (9) into the acceleration input gives the attitude history needed to create an arbitrary orbit.

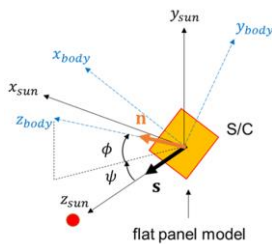


Fig. 3. Attitude angle.

Table 1. Solar sail properties.

Surface area $A$ [m <sup>2</sup> ]	16	
Mass $m$ [kg]	300	
Surface optical properties $C_*$ [-]	$C_{abs}$	0.163
	$C_{dif}$	0.118
	$C_{spe}$	0.719

Table 2. Parameters of orbits.

Semi-major axis $A_z$ [km]	14,000
Angular velocity [deg/day]	1.9895
Initial position $r_{RI}$ [m]	5
Spread speed $a_{RI}$ [-]	$3.435 \cdot 10^{-10}$
Chaser angular velocity $\omega_R$ [deg/day]	79.58

## 2.3 Reference and Relative Orbit

The orbit is determined arbitrarily within the range that can be expressed by the SRP, or attitude angle. The first step is to design a SCHO as a reference orbit. The SCHO requires control input to maintain, but for the purpose of obtaining a relative orbit suitable for interferometric observation, the control input for maintaining the orbit should be as small as possible. The SCHO is shown in Eq. (11). By setting the various parameters as shown in Table 2, the orbit can be maintained with minimal input.  $A_z$  is semi-major axis, and the smaller the radius, the smaller the input required to maintain the orbit. Therefore, it was set in consideration of the earth's shadow. In addition,  $\omega$  is the orbital angular velocity, which was determined by substituting Eq. (11) for  $y$  and  $z$  in Eq. (4) and solving it jointly.

$$\begin{aligned} x &= -A_x \cos(\omega t) + x_e \\ y &= \alpha A_x \sin(\omega t) \end{aligned} \quad (11)$$

$$\begin{aligned} z &= A_z \cos(\omega t) \\ \alpha &= \frac{\omega^2 + 1 + 2c_2}{2\omega} \end{aligned} \quad (12)$$

$$A_x = \frac{A_z}{\alpha}$$

$x_e$  represents the shift of the equilibrium point in consideration of SRP. Assuming that the angle is a small angle, there will be a constant SRP in the  $x$  direction, which can be expressed as Eq. (13).

$$x_e = -\frac{k_1}{1 + 2c_2} \quad (13)$$

The next step is to design the relative orbit. For interferometric observations, it is desirable to have an orbit with a continuously expanding formation size. This is because it is possible to collect various baseline vectors efficiently. Therefore, orbits were designed for each of

the two satellites with respect to the reference orbit as shown in Eqs. (14) and (15).

$$\begin{aligned} x_R &= 0 \\ y_R &= (r_R + a_R t) \sin(\omega_R t) \end{aligned} \quad (14)$$

$$\begin{aligned} z_R &= -(r_R + a_R t) \cos(\omega_R t) \\ x_R &= 0 \\ y_R &= -(r_R + a_R t) \sin(\omega_R t) \\ z_R &= (r_R + a_R t) \cos(\omega_R t) \end{aligned} \quad (15)$$

By superimposing these equations on the equations for the SCHO, the absolute orbits of the two satellites were designed.

$$\begin{aligned} x &= -A_x \cos(\omega t) + x_e \\ y &= \alpha A_x \sin(\omega t) + (r_{RI} + a_{RI} t) \sin(\omega_R t) \end{aligned} \quad (16)$$

$$\begin{aligned} z &= A_z \cos(\omega t) - (r_{RI} + a_{RI} t) \cos(\omega_R t) \\ x &= -A_x \cos(\omega t) + x_e \\ y &= \alpha A_x \sin(\omega t) - (r_{RI} + a_{RI} t) \sin(\omega_R t) \\ z &= A_z \cos(\omega t) + (r_{RI} + a_{RI} t) \cos(\omega_R t) \end{aligned} \quad (17)$$

By substituting Eqs. (16) and (17) for the orbits into Eqs. (6) and (7), the acceleration and attitude required to create the orbit can be obtained. However, it is difficult to follow the designed orbit even if it executes the attitude angle calculated in this way. Therefore, in this paper, LQR feedback control is applied.

### 3. Feedback Control

When the state vector is  $\mathbf{x} = [x \ y \ z \ \dot{x} \ \dot{y} \ \dot{z}]^T$  and the control vector is  $\mathbf{u} = [\psi \ \phi]^T$ , Eq. (4) together with Eq. (9) can be expressed as Eq. (18), where  $\mathbf{A}$  and  $\mathbf{B}$  are constant coefficient matrices containing  $c_2, k_1$ , and  $k_2$ .

$$\dot{\mathbf{x}} = \mathbf{A}\mathbf{x} + \mathbf{B}\mathbf{u} \quad (18)$$

The designed orbit is denoted as nominal orbit  $\mathbf{x}_{\text{nom}}$ , and the attitude angle used to create the orbit is denoted as nominal control  $\mathbf{u}_{\text{nom}}$ . The following Eq. (19) is obtained by subtracting these from Eq. (18).

$$\dot{\tilde{\mathbf{x}}} = \mathbf{A}\tilde{\mathbf{x}} + \mathbf{B}\tilde{\mathbf{u}} \quad (19)$$

$\tilde{\mathbf{x}} = \mathbf{x} - \mathbf{x}_{\text{nom}}$  and  $\tilde{\mathbf{u}} = \mathbf{u} - \mathbf{u}_{\text{nom}}$ , which represents the difference from the nominal. Here, an optimal regulator is introduced to minimize this difference. The optimal regulator minimizes the objective function as follows.

$$J = \int_0^{\infty} (\tilde{\mathbf{x}}^T \mathbf{R}_1 \tilde{\mathbf{x}} + \tilde{\mathbf{u}}^T \mathbf{R}_2 \tilde{\mathbf{u}}) dt \quad (20)$$

$\mathbf{R}_1$  and  $\mathbf{R}_2$  are constant symmetric matrices that represent the weights. In this case, the optimal feedback can be expressed as Eq. (21).

$$\tilde{\mathbf{u}} = -\mathbf{R}_2^{-1} \mathbf{B}^T \mathbf{P} \tilde{\mathbf{x}} \quad (21)$$

where  $\mathbf{P}$  is a matrix that satisfies the following Riccati equation.

$$\mathbf{P}\mathbf{A} + \mathbf{A}^T \mathbf{P} - \mathbf{P}\mathbf{B}\mathbf{R}_2^{-1} \mathbf{B}^T \mathbf{P} + \mathbf{R}_1 = 0 \quad (22)$$

Stabilize the orbit by adding the control quantity vector given by Eq. (21) to the feed-forward control quantity obtained in Chapter 2.3.

## 4. Simulation

In this chapter, the results of numerical simulations are presented to see if the design orbits shown in Chapter 2 can be realized by the control method. In this simulation, system dynamical equations are given in non-linear circular restricted three-body problem. The propagation time is set to 1 period of SCHO. The results are shown in Fig. 4 to 7.

First, Fig. 4 shows the orbit of the Chaser 1 satellite. It can be seen that SCHO is maintained. Next, Fig. 5 shows the relative orbit of Chaser 1, which also follows the orbit designed in Chapter 2. Finally, Figs. 6 and 7 show the attitude angle histories of the two satellites. It can be seen that the attitude angles of the satellites are represented by long period and short period oscillations. This indicates that long-period oscillation is necessary to maintain the orbit of SCHO and short-period oscillation is necessary to form a relative orbit. In any case, the values are realistic, and it can be said that this formation flight can be achieved only by the acceleration by SRP. However, the maximum angle is around 30 degrees, which threatens the assumption of small angle. The elimination of the small angle approximation is a future issue.

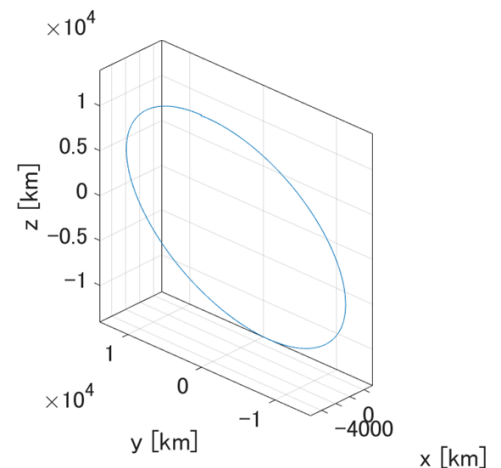


Fig. 4. The orbit of the Chaser 1.

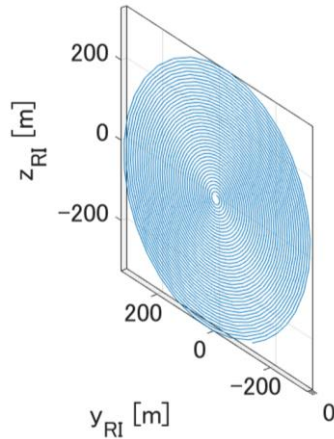


Fig. 5. Relative orbit.

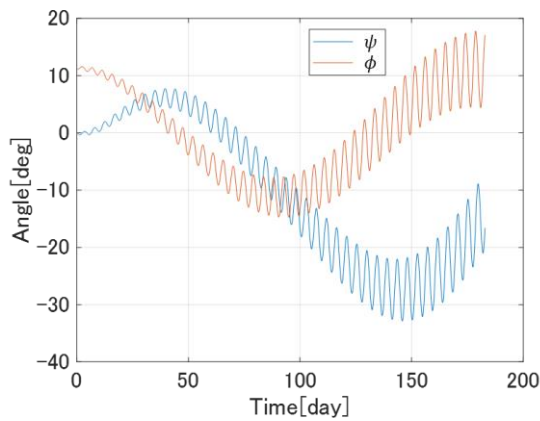


Fig. 6. The attitude angle history of Chaser 1.

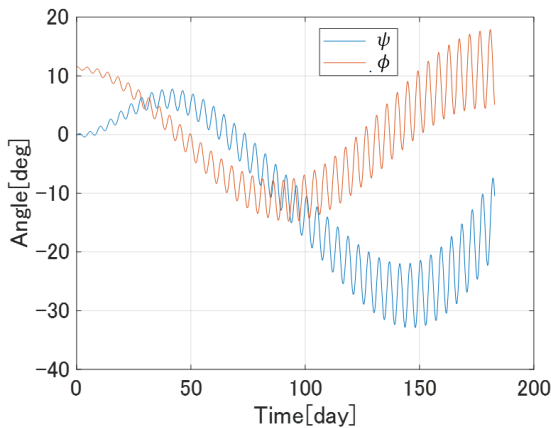


Fig. 7. The attitude angle history of Chaser 2.

## 5. Conclusion

In this paper, a formation flight suitable for interferometric observation in SCHO was designed. For the designed orbits, only SRP was used as a control input. It was confirmed that relative position control and station keeping were possible simultaneously. As a

control method, the SRP was changed by changing the attitude angle. In addition, LQR control was used for control.

As future work, it is necessary to design a control system that is closer to reality by not using the small-angle approximation and by solving the dynamics of the attitude and the orbit in a coupled manner.

## References

- [1] Bookless, J., and McInnes, C., Control of Lagrange Point Orbits Using Solar Sail Propulsion, *Acta Astronautica*, Vol. 62, No. 2, 2008, pp. 159-176.
- [2] Shahid, K., and Kumar, K. D., Formation Control at the Sun-Earth L2 Libration Point Using Solar Radiation Pressure, *Journal of Spacecraft and Rockets*, Vol. 47, No. 4, 2010, pp. 614-626.
- [3] Terao, K., and Kawaguchi, J., Design of Small Circular Halo Orbit around L2, *Proceedings of 15th Workshop on JAXA Astrodynamics and Flight Mechanics*, 2006, pp. 12-17.
- [4] Tanaka, K., and Kawaguchi, J., Small-amplitude Periodic Orbit around Sun-Earth L1/L2 Controlled by Solar Radiation Pressure, *The Japan Society for Aeronautical and Space Sciences*, Vol. 59, No. 1, 2016, pp. 33-42.
- [5] Tsuda, Y., Saiki, T., Funase, R., Modeling of Attitude Dynamics for IKAROS Solar Sail Demonstrator, *21st AAS/AIAA Space Flight Mechanics Meeting, AAS 11-112*, New Orleans, Louisiana, USA, 2011, pp. 147-162.